Aging of 1,ω-Alkyldithiol Interlinked Au Nanoparticle Networks

Yvonne Joseph,* Berit Guse,† and Gabriele Nelles

Materials Science Laboratory, Sony Deutschland GmbH, Hedelfinger Strasse 61, D-70327 Stuttgart, Germany

Received December 17, 2008

To identify the aging processes during long-term storage under different storage conditions, we investigated the composition of films comprising gold nanoparticles interlinked with 1,9-nonanedithiol and 1,16-hexadecanedithiol during a 44 month period using X-ray photoelectron spectroscopy (XPS). Additionally, we compared the initial structure and sensing properties toward toluene, 1-propanol, water, and hydrogen sulfide with the morphology and sensitivity after storage. Films stored under ambient conditions showed oxidation of sulfur and carbon and appearance of nitrogen, a significant loss of sulfur and the formation of larger particles in the film. The chemical selectivity of these films changed toward hydrophilic vapors and they became sensitive toward hydrogen sulfide. This is explained by the reaction of the thiol groups with ozone from the air, which destabilizes the network and significantly influences the particle/organic interface acting as sorption sites for gases. For films stored under argon only, an increase in free thiol groups in conjunction with a structural rearrangement of the film was observed. The selectivity of these films changed slightly toward hydrophilic analytes but they were still insensitive toward hydrogen sulfide.

Introduction

During the past few years, considerable progress has been made in understanding the functional properties of organically encapsulated metal nanoparticles.[1,2] Besides the investigation of their charge transport properties[3−12] their use as a chemical sensor was intensively studied[13−24] after pioneering work by Wohltjen and Snow.[25]

Despite the progress toward the qualitative understanding of the properties of these functional nanoparticle networks, the long-term aging behavior of these materials has not been investigated yet in detail, even if it is extremely important for their application. Recent studies on two-week-aged nanoparticulate surfaces showed that halide ions are critical for oxidation by air[26] and the processes as well as the time scale of aging are comparable with self-assembled monolayers (SAMs) on planar gold surfaces.[27] As encapsulated metal nanoparticles in general are often understood as the three-dimensional analogue of two-dimensional SAMs one should consider as well the aging behavior of the respective two-dimensional organic thiol monolayers on gold in laboratory air which was studied extensively in the past decade.[28] The main conclusion from these studies is that these SAMs are quickly oxidized by dilute atmospheric components, most likely ozone, especially when exposed to light. The observations interrelated with the oxidation process are the formation of oxidized sulfur species (sulfinates and sulfonates), a decreasing sulfur and carbon content, interpreted as partial desorption of the monolayer, and a structural rearrangement of the SAM.

Measuring the sorption properties of nanoparticle networks can give an insight into the properties of the materials on a molecular level. For nanoparticles interlinked with 1,ω-alkyldithiols, three possible sorption sites within the material were postulated:[13] Hydrophobic ("A") and hydrophilic parts ("B") of the organic matrix for respective sorption of hydrophobic and hydrophilic vapors and the particle surface("C") for sorption of gases. These sorption sites are illustrated in Figure 1. The sensing mechanism of chemiresistors coated with these materials has been explained by two counteracting effects: sorption-induced swelling of the

* Corresponding author. E-mail: Yvonne.Joseph @ eu.sony.com. Phone: 49(0) 711-5858-836. Fax: 49(0) 711-5858-99836.

† Current address: Product Development, tesa AG, Quickbornstrasse 24, 20253 Hamburg.

(1) Shipway, A. N.; Katz, E.; Willner, I. *ChemPhysChem* **2000**, *1*, 18–52.
(2) Daniel, M.-C.; Astruc, D. *Chem. Rev.* **2004**, *104*, 293–346.
(3) Trudeau, P. E.; Kwan, E.; Orozco, A.; Dhirani, A.-A. *J. Chem. Phys.* **2002**, *117*, 3978–3981.
(4) Trudeau, P. E.; Escorcia, A.; Dhirani, A. A. *J. Chem. Phys.* **2003**, *119*, 5267–5273.
(5) Zabet-Khosousi, A.; Trudeau, P. E.; Suganuma, Y.; Dhirani, A. A. *Phys. Rev. Lett.* **2006**, *96*, 156403−1156403−4.
(6) Pelka, J. B.; Brust, M.; Gierlowski, P.; Paszkowicz, W.; Schell, N. *Appl. Phys. Lett.* **2006**, *89*, 063110−1063110−3.
(7) Terril, R. H.; Postlethwaite, T. A.; Chen, C. H.; Poon, C. D.; Terzis, A.; Chen, A.; Hutchison, J. E.; Clark, M. R.; Wignall, G.; Londono, J. D.; Superfine, R.; Falvo, M.; Johnson Jr, C. S.; Samulski, E. T.; Murray, C. *J. Am. Chem. Soc.* **1995**, *117*, 12537–12548.
(8) Wuelfing, W. P.; Green, S. J.; Pietron, J. J.; Cliffel, D. E.; Murray, R. W. *J. Am. Chem. Soc.* **2000**, *122*, 11465–11472.
(9) Zamborini, F. P.; Leopold, M. C.; Hicks, J. F.; Kulesza, P. L.; Malik, M. A.; Murray, R. W. *J. Am. Chem. Soc.* **2002**, *124*, 8958–8964.
(10) Müller, K. H.; Wei, G.; Raguse, B.; Myers, J. *Phys.Rev.B* **2003**, *68*, 155407−1155407−6.
(11) Schmid, G.; Simon, U. *Chem. Commun.* **2005**, *697*, 710.
(12) Bernard, L.; Kamdzhilov, Y.; Calame, M.; Van der Molen, S. J.; Liao, J.; Schoenenberger, C. *J. Phys. Chem. C* **2007**, *111*, 18445–18450.
(13) Joseph, Y.; Guse, B.; Yasuda, A.; Vossmeyer, T. *Sens. Actuators, B* **2004**, *98*, 188–195.
(14) Park, S.-J.; Taton, T. A.; Mirkin, C. A. *Science* **2002**, *295*, 1503–1506.
(15) Han, L.; Daniel, D. R.; Maye, M. M.; Zhong, C.-J. *Anal. Chem.* **2001**, *73*, 4441–4449.

10.1021/cm803407n CCC: $40.75
Published on Web 03/19/2009

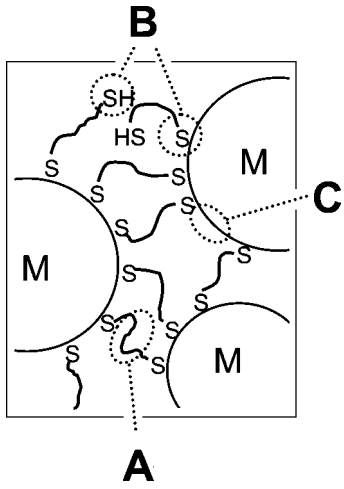

Figure 1. Model illustrating three possible sorption sites in a nanoparticle network. "A" are hydrophobic parts of the organic matrix, "B" are hydrophilic parts of the organic matrix, and "C" are organic-free parts of the particle surface.

material leading to an increase of the resistance, and a permittivity change in the surrounding organic matrix resulting in a decrease of the resistance. On the basis of these insights, different influences on the sensitivity and selectivity of the sensors were identified and used to tailor the sensor responses: Implementation of or change in functional groups in the organic matrix or change in the composition of the nanoparticles led to changed sorption properties and thus different selectivity.[13,29,30] In addition, increasing the length of flexible linkers increases the sensitivity of the sensor because of a better ability to swell,[31−34] whereas using a rigid linker prohibits swelling, resulting in mainly permittivity change induced signals.[35] It was additionally shown that the film morphology has a dramatic influence on the sensitivity of the device because of different swelling behavior.[36]

Here we will present an investigation of the composition of nanoparticle networks comprising 4 nm gold nanoparticles interlinked with 1,16-hexadecanedithiol (AuC16) or 1,9-nonanedithiol (AuC9) using X-ray Photoelectron Spectroscopy (XPS) aged over 44 months to identify processes occurring during long-term storage under different storage conditions. Additionally we compared the initial morphology using scanning electron microscopy (SEM) and responses toward toluene, 1-propanol, water, and hydrogen sulfide with the structure and sensitivity of all samples after the storage. The analytes serve as model analytes for hydrophobic and hydrophilic vapors and gases to monitor the different sorption sites "A", "B", and "C" explained in Figure 1 to get an insight into the chemistry in the molecular level. The investigation on 1,16-hexadecanedithiol interlinked films is presented in the following while the results of films using 1,9-nonanedithiol as interlinking organic component, confirming the same trends, are given in the Supporting Information (Figure S1−S5).

Experimental Section

Materials. All used chemicals with reagent grade or higher quality were purchased from Merck, ABCR, or Sigma-Aldrich and used as received. The synthesis of the 1,16-hexadecanedithiol is described elsewhere.[31] Au nanoparticles with a dodecylamine stabilizing shell were prepared in a similar way as described by Leff et al.[37] and Brust et al.,[38] resulting in particles with a core diameter of ∼4 ± 1 nm.[31]

Film Preparation. The films were prepared based on the method described by Bethell et al.[39] on oxidized silicon wafer substrates equipped with three interdigitated gold electrode structures each (50 finger pairs, 5 μm width and 100 nm height, 5 μm spacing, 900 μm overlap; Institut für Mikrotechnik Mainz GmbH, Mainz, Germany). The cleaning and silanization of the substrates is described elsewhere.[31] The films were deposited via layer-by-layer self-assembly under ambient conditions (∼22 °C, ∼35% rh) using Au nanoparticles and 1,9-nonanedithiol (C9) or 1,16-hexadecanedithiol (C16) as linker molecule. The concentration of the Au nanoparticles was adjusted to an absorbance of 0.4 at the maximum of the plasmon band (λ_{max} = 514 nm with a 2 mm path length) whereas the concentration of the linker solution was 5 mM. The cleaned and silanized substrates were placed 14 times for 15 min alternating into the Au nanoparticle solution and into the linker solution. To avoid a precipitation of the material in the solutions, the samples were rinsed in toluene baths between each solution.

Film Storage. After preparation the samples were stored in 1.5″ transparent polypropylene wafer boxes (Entegris, Inc., Chaska, Minnesota, USA) under the following conditions (one substrate each): (a) under ambient conditions, exposed to light ("ambient/light"); (b) under ambient conditions, wrapped in aluminum foil ("ambient/dark"); (c) under Ar in a glovebox, exposed to light ("inert/light"); (d) under Ar in a glovebox, wrapped in aluminum foil ("inert/dark"). The samples were transported to the instruments for measurements under ambient conditions, but the exposure time to air and light was tried to be kept as short as possible (less than 15 min).

X-ray Photoelectron Spectroscopy (XPS). The chemical composition of the films was investigated with a Kratos Axis Ultra system equipped with a DLD detector, a monochromated Al Kα X-ray source and a charge neutralizer. The pass energy of the analyzer was set to 20 eV and the power of the X-ray source to 150 W. To avoid radiation induced damage, we selected a fresh spot on the samples for each series of spectra. To compensate long-

(16) Zhang, H.-L.; Evans, S. D.; Henderson, J. R.; Miles, R. E.; Shen, T.-H. *Nanotechnology* **2002**, *13*, 439–444.
(17) Evans, S. D.; Johnson, S. R.; Cheng, Y. L.; Shen, T. *J. Mater. Chem.* **2000**, *10*, 183–188.
(18) Vossmeyer, T.; Guse, B.; Besnard, I.; Bauer, R. E.; Muellen, K.; Yasuda, A. *Adv. Mater.* **2002**, *14*, 238–242.
(19) Grate, J. W.; Nelson, D. A.; Skaggs, R. *Anal. Chem.* **2003**, *75*, 1868–1879.
(20) Convertino, A.; Capobianchi, A.; Valentini, A.; Cirillo, E. M. *Adv. Mater.* **2003**, *15*, 1103–1105.
(21) Cai, Q.-Y.; Zellers, E. T. *Anal. Chem.* **2002**, *74*, 3533–3539.
(22) Zamborini, F. P.; Leopold, M. C.; Hicks, J. F.; Kulesza, P. J.; Malik, M. A.; Murray, R. W. *J. Am. Chem. Soc.* **2002**, *124*, 8958–8964.
(23) Haick, H. *J. Phys. D: Appl.Phys.* **2007**, *40*, 7173–7186.
(24) Drake, C.; Deshpande, S.; Bera, D.; Seal, S. *Int. Mater. Rev.* **2007**, *52*, 289–317.
(25) Wohltjen, H.; Snow, A. W. *Anal. Chem.* **1998**, *70*, 2856–2859.
(26) Dasog, M.; Scott, W. J. *Langmuir* **2006**, *23*, 3381–3387.
(27) Vericat, C.; Benitez, G. A.; Grumelli, D. E.; Vela, M.; Salvarezza, R. C. *J. Phys.: Condens. Matter* **2008**, *20*, 184004-(8p).
(28) Willey, T. M.; Vance, A. L.; van Buuren, T.; Bostedt, C.; Terminello, L. J.; Fadley, C. S. *Surf. Sci.* **2005**, *576*, 188–196.
(29) Vossmeyer, T.; Joseph, Y.; Besnard, I.; Harnack, O.; Krasteva, N.; Guse, B.; Nothofer, H.-G.; Yasuda, A. *SPIE Proc.* **2004**, *5513*, 202–212.
(30) Krasteva, N.; Besnard, I.; Guse, B.; Bauer, R. E.; Müllen, K.; Yasuda, A.; Vossmeyer, T. *Nano Lett.* **2002**, *2*, 551–555.
(31) Joseph, Y.; Besnard, I.; Rosenberger, M.; Guse, B.; Nothofer, H. G.; Wessels, J.; Wild, U.; Knop-Gericke, A.; Su, D.; Yasuda, A.; Vossmeyer, T. *J. Phys. Chem. B* **2003**, *107*, 7406–7413.

term variations of the spectrometer, we normalized the intensities of the spectra to the background at the higher binding energy side of the respective spectrum of the freshly prepared sample. From all spectra, a linear background was subtracted and the binding energy was calibrated to Au 4f = 84.0 eV. The spectra were fitted using Voigt profiles (30% Lorentz, 70% Gauss) with the spin orbit splitting for S 2p set to 1.18 eV. The intensity ratio was kept at 2:1 (S $2p_{3/2}$:S $2p_{1/2}$).

Scanning Electron Microscopy (SEM). The film morphology was characterized using a Leo Gemini 1530 field emission scanning electron microscope. The samples were contacted to the sample holder with silver paint and conducting carbon pads to prevent charging in the SEM. The images were acquired using an Inlens detector.

Sensor Measurements. The vapor tests were performed by dosing the samples with 5000 ppm toluene, 1-propanol, and water. Here, the same instruments as described in ref 31 were used to perform in situ resistance measurements. For hydrogen sulfide generation, a Kin-Tek 491-M permeation system (Kin-Tek Laboratories, Inc., LaMarque, Texas, USA) equipped with a hydrogen sulfide permeation tube (emission rate: 358 ng/min@40 °C) was used. Catalytically purified and dried air was used as carrier gas, and all experiments were carried out at room temperature. The resistances of the chemiresistors were monitored with an applied bias of 100 mV. The sensor signal is expressed as the relative differential resistance response the, i.e., change in resistance ΔR divided by the baseline resistance R_{ini}.

Results

Thin nanoparticulate films were prepared on substrates equipped with interdigitated electrode structures. The samples were stored over 44 months under ambient/light, ambient/dark, inert/light, and inert/dark conditions afterward. To study the processes responsible for aging of the material, we performed XPS measurements of all samples at intervals during the storage. Spectra of gold, sulfur, and carbon originating from the film material itself, and of oxygen and nitrogen due to suspected impurities, were recorded each time. To reveal possible additional impurities, we measured survey spectra but never found unexpected signals.

The S 2p spectra of the films stored under ambient/light conditions are given in Figure 2. The spectrum of the freshly prepared sample is dominated by two species. At 162.1 eV thiols bound to gold (thiolates) and at 163.5 unbound thiols are observed.[40,41] During storage, the amount of both species

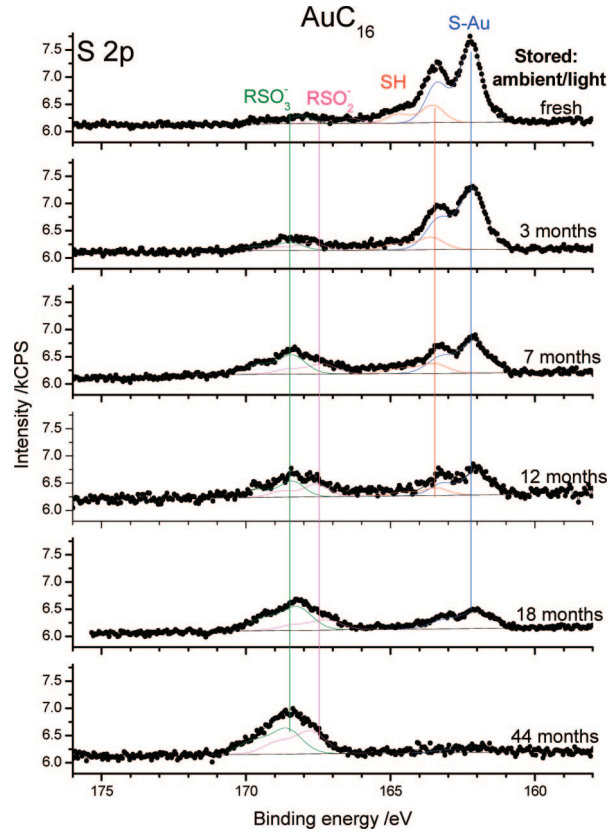

Figure 2. S 2p XP spectra of AuC16 stored under ambient/light conditions during 44 months.

decreased while two new species appeared and increased continuously with storage time. According to their binding energies they can be attributed to oxidized sulfur species, in particular sulfinates (167.4 eV) and sulfonates (168.5 eV).[28] In the final spectrum of the sample aged for 44 months in ambient/light conditions, almost mere oxidized sulfur species are present. In addition, the total amount of sulfur (represented by the area under the spectrum) was significantly reduced, indicating loss of sulfur during aging under ambient conditions. The trends within the ambient/dark spectra are comparable with those of the ambient/light sample, but the oxidation was slower in the first year.

The S 2p spectra of the inert/light stored sample are given in Figure 3. The initial spectrum is very similar to the initial one given in Figure 2, demonstrating the reproducibility of sample preparation. However, in contrast to the ambient stored samples, films stored under inert conditions showed neither a decrease in the sulfur content nor a pronounced formation of oxidized sulfur species. Mainly a continuous change of the relative ratio of thiolates to free thiol species was observed. The spectra of the films stored under inert conditions were very similar regardless of storage under light or dark conditions as shown in Figure S2 (Supporting Information).

For further comparison, the initial and final C 1s, N 1s, O 1s, and Si 2s spectra after storage are presented below to reveal the influences of aging on the elemental composition under the different storage conditions. All C 1s spectra given in Figure 4 are very similar with the main species at 284.6 eV, which can be attributed to aliphatic carbon. However,

(32) Krasteva, N.; Guse, B.; Besnard, I.; Yasuda, A.; Vossmeyer, T. *Sens. Actuators, B* **2003**, *92*, 137–143.
(33) Krasteva, N.; Fogel, Y.; Bauer, R.; Müllen, K.; Joseph, Y.; Matsuzawa, N. N.; Yasuda, A.; Vossmeryer, T. *Adv.Funct.Mater.* **2007**, *17*, 881–888.
(34) Wang, L.; Shi, X.; Kariuki, N. N.; Schadt, M.; Wang, G. R.; Rengdeng, Q.; Choi, J.; Luo, J.; Lu, S.; Zhong, C.-J. *J. Am. Chem. Soc.* **2007**, *129*, 2161–2170.
(35) Joseph, Y.; Peic, A.; Chen, X.; Michl, J.; Vossmeyer, T.; Yasuda, A. *J. Phys. Chem. C* **2007**, *111*, 12855–12859.
(36) Joseph, Y.; Guse, B.; Vossmeryer, T.; Yasuda, A. *J. Phys. Chem. C* **2008**, *112*, 12507–12514.
(37) Leff, D. V.; Brandt, L.; Heath, J. R. *Langmuir* **1996**, *12*, 4723–4730.
(38) Brust, M.; Walker, D.; Bethell, D.; Schiffrin, D. J.; Whyman, R. *Chem. Commun.* **1994**, *7*, 801–802.
(39) Bethell, D.; Brust, M.; Schiffrin, D. J.; Kiely, C. *J. Electroanal. Chem.* **1996**, *409*, 137–143.
(40) Bourg, M. C.; Badia, A.; Lennox, R. B. *J. Phys. Chem. B* **2000**, *104*, 6562–6567.
(41) Castner, D. G. *Langmuir* **1996**, *12*, 5083–5086.

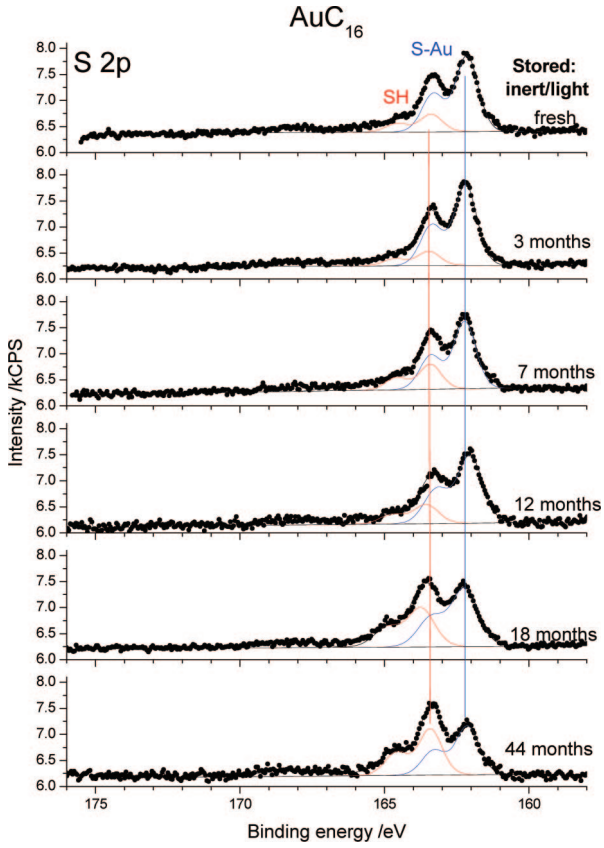

Figure 3. S 2p XP spectra of AuC16 stored under inert/light conditions during 44 months.

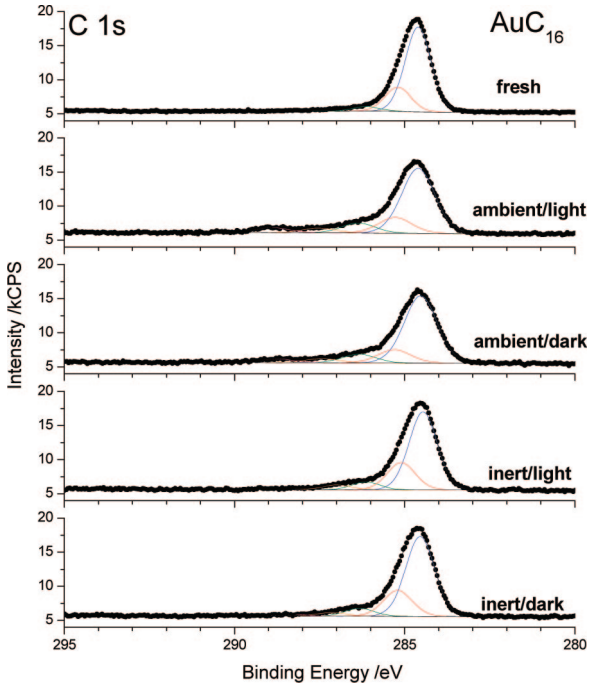

Figure 4. C 1s XP spectra of AuC16 stored for 44 months under the indicated conditions.

careful observation reveals a slightly higher amount of oxidized carbon at the high binding energy side around 288−289 eV, most likely C═O, for ambient stored samples, which is not observed under inert storage.

The N 1s XP spectra are given in Figure 5. The initial spectrum shows no nitrogen signal indicating that all

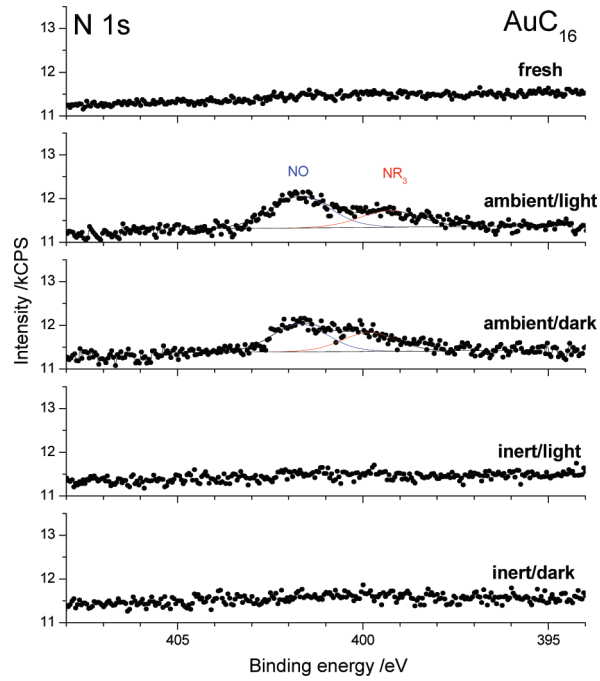

Figure 5. N 1s XP spectra of AuC16 stored for 44 months under the indicated conditions.

dodecylamine ligands protecting the particles after synthesis were exchanged by 1,ω-alkyldithiol linker molecules during film assembly. Although the nanoparticle networks stored under inert conditions were still nitrogen-free after 44 months, the ambient stored samples contained significant amounts of nitrogen. In the respective spectra, two species can be identified. Around 399.5 eV, a minor species is found that can be attributed to amines or amides, whereas the species around 401.7 eV is presumably due to NO. These two species are most likely sorbed from the surrounding air during storage under ambient conditions.

Figure 6 shows the O 1s spectra before and after storage. The initial spectrum already exhibits a very small amount of oxygen that may be due to oxidative processes during film preparation. Films stored under ambient conditions reveal evolving oxygen peaks indicative of oxidized sulfur (531.8 eV) and carbon (533.4). Also, for the inert stored films, oxygen signals are observed. However, they appear at a different position (532.2 eV) and are most likely due to silicon dioxide.[42] This assumption is supported by the Si 2s spectra in Figure 7. Clear silicon signals are present for the films stored under inert conditions, while for the initial and ambient stored films, no Si can be detected. In the latter case, the film thickness is obviously larger than the information depth of the method, whereas in the case of the inert stored sensors, the substrate becomes visible. One reason may be a structural reorganization accompanied by hole or crack formation in the film.

To detect such changes in film morphology, we measured the samples by scanning electron microscopy (SEM). Representative SEM images are shown in Figure 8. The initial film was very homogeneous and showed small particles.

(42) Seyama, H.; Soma, M. *J. Chem. Soc., Faraday Trans. 1* **1985**, *81*, 485–495.

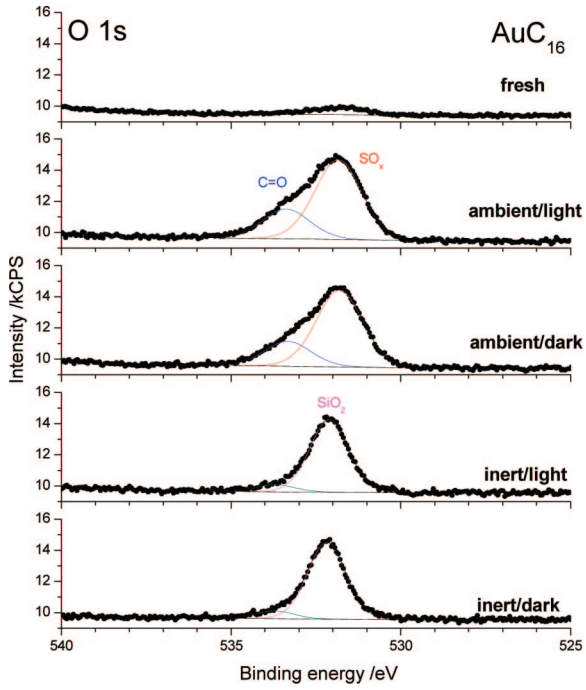

Figure 6. O 1s XP spectra of AuC16 stored for 44 months under the indicated conditions.

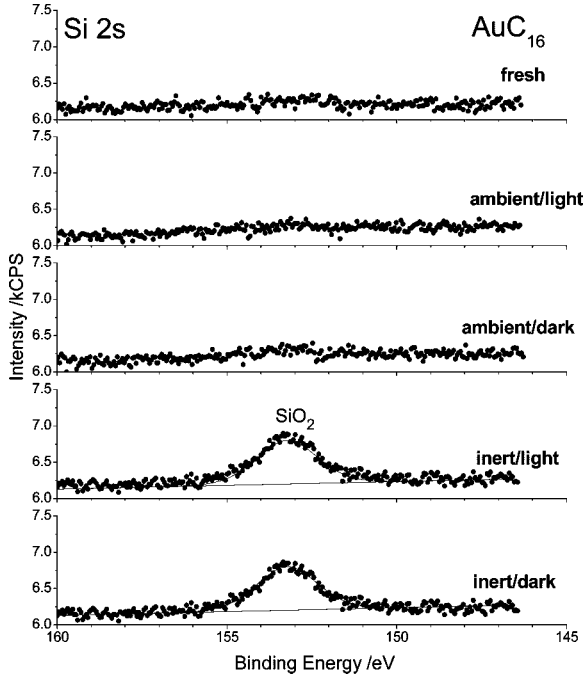

Figure 7. Si 2s XP spectra of AuC16 stored for 44 months under the indicated conditions.

After the film was stored under ambient conditions, it was still homogeneous, but the particle size increased significantly. Inert storage conditions did not change the particle size, whereas the film morphology became rougher on the nanometer scale.

As the substrates were equipped with interdigitated electrodes, the XPS results are complemented with resistance measurements as well as with an investigation on the sensitivity toward toluene 1-propanol, water, and hydrogen sulfide to monitor changes of the sorption sites. The initial mean values of the resistances of the AuC16 films are compared with the mean resistances after storage in Table 1. Before storage, all 12 chemiresistors had comparable resistances within a relative error of less than 9%, demonstrating again the good reproducibility of the device preparation. After storage under ambient conditions, the resistances strongly decreased, whereas the samples stored under an inert atmosphere maintained their initial high resistance. In both cases, the resistances of the samples stored under daylight conditions were lower than those of the samples stored under dark conditions.

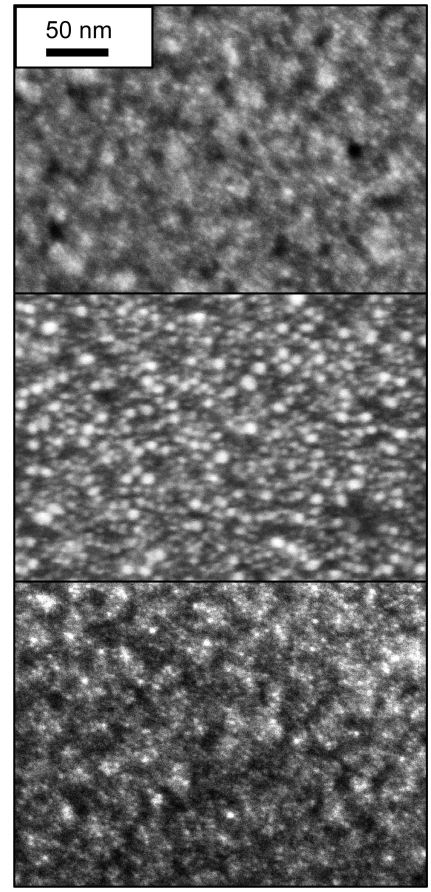

Figure 8. SEM images of AuC16: (top) initial film; (middle) film stored under ambient light conditions; and (bottom) film stored under inert light conditions.

Table 1. Mean Values of Initial and Final Resistances of Three AuC16 Chemiresistors before and after Storage for 44 Months

storage conditions	initial resistance (kΩ)	final resistance (kΩ)
ambient, light	314.7 ± 28.0	5.2 ± 1.6
ambient, dark	317.7 ± 17.8	21.2 ± 4.5
inert, light	313.3 ± 9.5	255.0 ± 9.6
inert, dark	308.7 ± 22.1	287.3 ± 8.5

The responses of the AuC16 networks toward 5000 ppm toluene, 1-propanol, water, and 50 ppb hydrogen sulfide before and after storage are shown in Figure 9. The results clearly show that all chemiresistors were still active after 44 months but with a changed sensitivity and selectivity to the indicated analytes. The films stored under argon showed in each case a smaller change than those stored under ambient conditions, and their responses were very similar when comparing dark and light inert storage conditions.

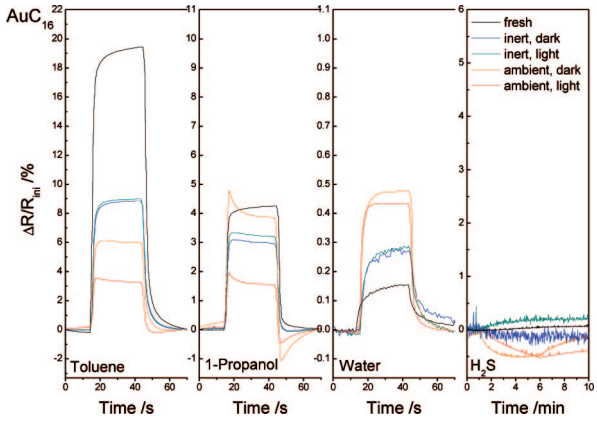

Figure 9. Responses of AuC16 sensors before and after storage toward 5000 ppm of toluene, 1-propanol, and water and 50 ppb of hydrogen sulfide. The storage conditions are indicated.

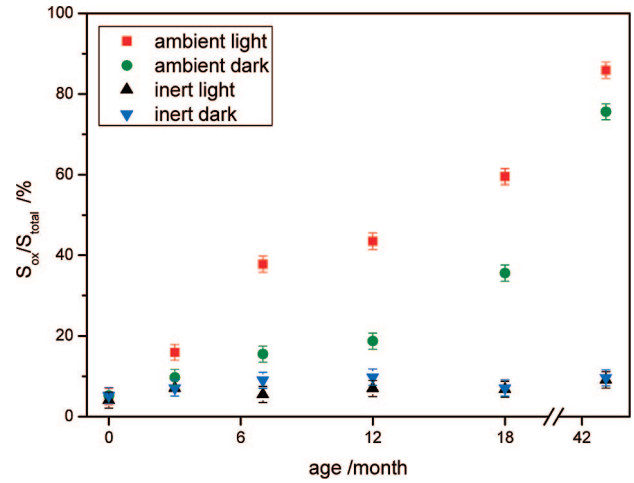

Figure 10. Oxidized sulfur content in dependence of the storage time under different conditions.

For toluene, which interacts with the hydrophobic chains in the sensor material, i.e., sorption sites "A", all responses were strongly decreased during storing, whereas for water, which interacts with the sorption sites "B", a clear increase was be observed. 1-Propanol appears to interact with both sorption sites because the responses decrease only slightly. Interestingly, the signal shape of the samples stored under ambient conditions changed from almost rectangular toward "fish tailing", whereas the films stored under inert conditions change their shape only slightly. Such "fish tailing" behavior was already observed earlier mainly for hydrophilic vapors, but no explanation has yet been found.

The fresh AuC16 film was not sensitive toward hydrogen sulfide, which should adsorb on the particle surface and thus give information on the sorption sites "C". However, films stored under ambient conditions gave clear responses toward 50 ppb of the analyte, whereas the argon-stored sensors remained insensitive.

The same trends in the results for AuC16 were also observed for AuC9, as shown in the Supporting Information.

Discussion

The main aging process during ambient storage of gold nanoparticles interlinked with organic dithiols is the oxidation of the sulfur of the interlinking molecule as confirmed by XPS. Upon storage, oxidation processes show a clear impact on the thiol-mediated particle/organic interface contact. Because the sulfinates and sulfonates are not as strongly bound to the nanoparticles surface as the initial thiols,[43] the organic partly desorbs. This implies that the nanoparticles are no longer completely protected so that the particles coalesce, leading to an increased particle size as observed by SEM. The change in particles size is also reflected by the decrease in the resistance of the material with storage time. Concerning the sensing properties of the ambient aged nanoparticle network, desorption of the oxidized organic molecules leads to a decrease of the sorption sites "A" and "B". Additionally, the oxidation reaction changes the nature of the remaining sorption sites "B" from thiols to more hydrophilic SO_x functionalities. This changes the selectivity of the material from hydrophobic to more hydrophilic, which can be nicely observed for the sorption of toluene and water. The change in the sites "B" also changes the kind of interaction of the nanoparticle network with analytes, which may explain the observed fishtailing behavior in the 1-propanol responses. The increase in particle size as well as changes in the particle/organic interface influence the sorption sites "C". The surface of the particles becomes accessible for sorption of impurities from the air, like the observed nitrogen species, or analytes dosed on purpose, like hydrogen sulfide.

During inert storage, XPS revealed a higher amount of free thiols in the film as well as the appearance of substrate signals. Both observations indicate a structural rearrangement in the nanoscale regime, which was also visible by SEM. This means that the particle organic interface remains unchanged but the film morphology is transformed. As was recently shown,[36] the sensor signal is influenced by the morphology of the film. An island like morphology results in a more negative response than a homogeneous film, which is observed in the sensor measurement for toluene. The increased response to water indicates that the films become more hydrophilic. This is most likely due to the fact that some of the sorption sites "B" change from thiolates to free thiols. As the sorption sites "C" are obviously unchanged, the film is still insensitive toward hydrogen sulfide.

To reveal the best storage conditions for thiol-stabilized gold nanoparticles, the time dependence of the oxidation process in this study for different storage conditions is shown in Figure 10. For ambient conditions, especially in the first year, the film oxidation is slower when the films are stored in a dark environment compared to films stored under light conditions. However, they will presumably both reach the same state of oxidation at very long storage time. Storage under inert conditions prevents the oxidation independently on light exposure but the film morphology will change. Nevertheless, the absolute time scale of the described processes may differ on exact storage conditions like packaging, ambient ozone content, or light exposure and on

(43) Garrell, R. L.; Chadwick, J. E.; Severance, D. L.; McDonald, N. A.; Myles, D. C. *J. Am. Chem. Soc.* **1995**, *117*, 11563–11571.

film properties like particle size and structure or the nature of the organic molecule.

Conclusions

The processes of aging of 1,ω-alkyldithiol-interlinked nanoparticle networks under different storage conditions over 44 months have been identified by XPS and SEM. Under ambient conditions, mainly oxidation of the thiols occurs followed by secondary processes like alkylsulfonate desorption and coalescence of particles, whereas under inert storage, oxidation does not occur but the morphology of the film changes.

The observed changes in the film were correlated to changes in the sorption properties of the materials by discussing the influence of aging on the sorption sites in the sensor film. These results confirm the postulated sorption sites and also show that aging has a major influence on the sensing properties. Consequently, all values of sensor results based on Au-nanoparticle/thiol materials have to be interpreted with regard to aging effects.

To clarify the time scale of the described reactions, influenced by storage conditions like packaging, ozone content, or light exposure or by film properties like particle size and structure or the nature of the organic molecule as well as chemical response effects like fishtailing, we require more detailed studies and all of these factors have to be considered for usage and storage of nanoparticle/thiol-based devices.

Acknowledgment. The authors thank Nadejda Krasteva, Isabelle Raible, Florian von Wrochem, Tobias Vossmeyer, Akio Yasuda, and William Ford for fruitful discussions.

Supporting Information Available: The results of films using 1,9-nonanedithiol as interlinking organic component (Figures S1−S5) (PDF). This material is available free of charge via the Internet at http://pubs.acs.org.

CM803407N